33rd Annual International Conference of the IEEE EMBS
Boston, Massachusetts USA, August 30 - September 3, 2011

Electromagnetic Drive of Microrobot Geometrically Constrained in Blood Vessel

S. Nakamura, K. Harada, *Member, IEEE* , N. Sugita,
M. Mitsuishi, *Member, IEEE*, and M. Kaneko, *Fellow, IEEE*

***Abstract*— We propose new electromagnetic actuation of a microrobot by utilizing geometric constraints in a blood vessel. In our concept, a microrobot travels in a vascular network while keeping the contact to the vascular wall. In the paper, forces working on the microrobot are modeled in two dimensions, and conditions to propel the microrobot while pushing it against the vascular wall are described. The design of the microrobot composed of three permanent magnets is also presented. The feasibility of the 2D actuation of the microrobot was confirmed using an experimental setup composed of four pairs of coils generating both uniform magnetic fields and uniform magnetic field gradients. Finally, the model was extended to 3D in order to investigate 3D actuation of the microrobot.**

I. Introduction

MICROROBOTS have been studied to develop diagnostic or interventional devices working in small spaces in a minimal invasive manner. For example, electromagnetically-driven intraocular microrobots [1], microrobots working in MRI [2] have been studied, as other microrobots are summarized in the review article [3]. The previous studies about microrobotic control are about microrobotic driving methods in a static liquid except few examples [4], and this is because the control in a flowing liquid is challenging. Unlike other robots, microrobots are moved by wireless control, and thus microrobots in a flow can be easily affected by the turbulence of the flow, making the control difficult.

The goal of our research is to develop microrobots and their control in flowing liquid, i.e. blood. Since the vascular network covers most part of the body, microrobots which can be controlled in flowing liquid would lead to practical applications including therapeutic microrobots for the embolism of cerebral aneurysm or for destroying blood clots, and drug-delivery microrobots.

In this paper, we propose the design of microrobot and its control using electromagnetic drive. In the proposed method, the microrobot can move along blood vessel allowing contact with the vascular wall. In this paper, force and torque applied to the microrobot working in flowing liquid were modeled in 2D, and an experimental setup using four pairs of coils was developed to demonstrate the feasibly of the proposed control method. Thereafter, the model was extended to 3D.

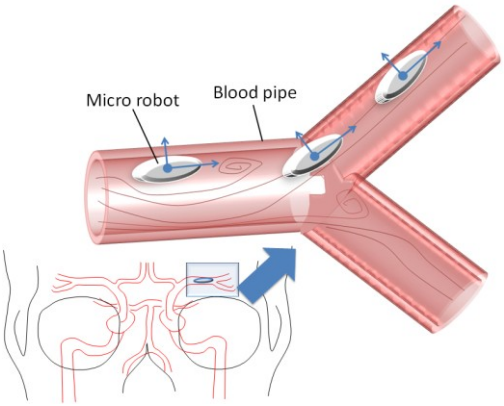

Fig. 1 Concept of the electromagnetic drive of a microrobot moving along a blood vessel

II. Method of Electromagnetic Drive

A. Concept of Electromagnetic Drive

Figure 1 shows our concept of the electromagnetic drive of a microrobot moving along blood vessel. Thanks to the geometric constraints allowing the microrobot to be in contact with the vascular wall, the position of the microrobot can be controlled only with 3-DOF positioning, whereas 6-DOF control is necessary in a free space. By reducing the number of control parameters, we can achieve simple control of microrobots with robustness against fluidic disturbance.

B. Two-dimensional Geometric Constraint

Figure 2 shows the 2D model of the force and torque working on a microrobot placed on a vascular wall. **F** is induced magnetic force on the microrobot, $\mathbf{F}_f$ is fluid force, and m**g** is gravity force. **T** and $\mathbf{T}_f$ are induced torques working on a microrobot by external magnetic field and fluid force, respectively. By implementing fluid force to the 2D model, the conditions where the microrobot moves along the vascular wall while being touched to the wall are obtained. The conditions are described as:

$$\left(\mathbf{F}+m\mathbf{g}+\mathbf{F}_f\right)\cdot\mathbf{e}_x-\mu(\mathbf{F}+m\mathbf{g}+\mathbf{F}_f)\cdot\mathbf{e}_y>0 \quad (1)$$

$$(\mathbf{F}+m\mathbf{g}+\mathbf{F}_f)\cdot\mathbf{e}_y>0 \quad (2)$$

$$\mathbf{T}+\mathbf{T}_f-(\mathbf{F}+m\mathbf{g}+\mathbf{F}_f)\times\mathbf{R}_a>\mathbf{0} \quad (3)$$

$$\mathbf{T}+\mathbf{T}_f-(\mathbf{F}+m\mathbf{g}+\mathbf{F}_f)\times\mathbf{R}_b<\mathbf{0} \quad (4)$$

Manuscript received March 26, 2011.

S. Nakamura, K. Harada, N. Sugita and M. Mitsuishi are with the Department of Mechanical Engineering, The University of Tokyo, Bunkyo-ku, Tokyo, 113-8656 Japan. (Tel and Fax: +81-3-5841-6357; e-mail: nakamura@ nml.t.u-tokyo.ac.jp).

M. Kanako is with the Department of Mechanical Engineering, Osaka University, Suita, Osaka, 565-0871 Japan.

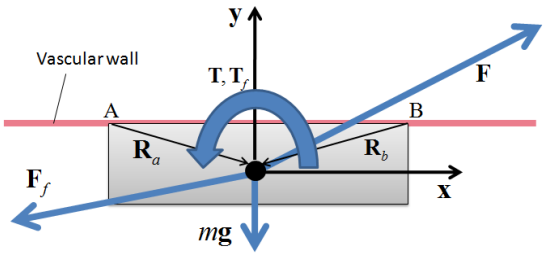

Fig. 2 Two-dimensional model of micro robot placed on vascular wall with applied external magnetic force/moment and fluid force

where μ is a static friction coefficient, and $\mathbf{e}_i$ is the unit vector in the i axis. Equation (1) expresses the condition where the microrobot moves in the positive direction of the x axis; the magnetic force in the x axis needs to be stronger than the resultant force by the drag force and static friction. Equation (2) - (4) denotes the condition to keep the microrobot touched to the vascular wall. As described in (2), the magnetic force in the y axis needs to be stronger than the resultant force by the gravity and lifting force in the y axis. Equation (3) and (4) are to prevent the microrobot from rotating about the point A or B. By satisfying these equations, we can move the microrobot to a desired location, using the force to push the microrobot against the wall, propulsion force to move it along the wall and torque to keep the microrobotic posture parallel to the wall.

C. Design of Microrobot

To apply both the force pushing the microrobot against the vascular wall and the propulsion force, we propose the design of the microrobot composed of three permanent magnets as shown in Fig. 3. Two permanent magnets which are identical in shape and magnetization were attached to the both ends of the central magnet so that the magnetized direction of the side magnets was orthogonal to that of the central magnet. Force working on a ferromagnetic body, in unit N, is described as:

$$\mathbf{F} = V(\mathbf{M} \cdot \nabla)\mathbf{B} = V\mathbf{M} \cdot (\nabla \mathbf{B}) \qquad (5)$$

where V, **B**, and **M**, are the volume of the body in unit m^3, the flux density of an external magnetic field in unit T, and magnetization in unit A/m, respectively. As shown in Fig. 3, the total magnetic moment V**M** consists of two components; the moment orthogonal to the vascular wall and the moment along the wall. The combination of three permanent magnets resulted in these components.

The torque working on a magnetized body is expressed as:

$$\mathbf{T} = V\mathbf{M} \times \mathbf{B} \qquad (6)$$

As the torque tends to align the magnetic moment to the external magnetic field, an external magnetic field which coincides with the direction of the magnetic moment can keep the microrobot in contact with the vascular wall while adding propulsion force.

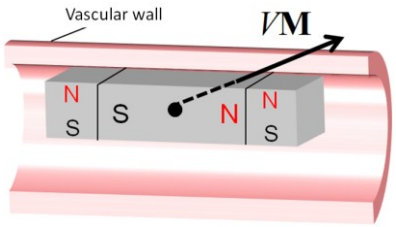

Fig. 3 Total magnetic moment of the microrobot consisting of three permanent magnets for moving along the blood vessel

III. Experiment of Two-Dimensional Drive

A. Experimental Setup

An experimental setup using four pairs of coils was developed to achieve 2D motion of the microrobot for feasibility study. Fluid is not used in the experiment because the purpose of this experiment is to investigate the concept of the microrobotic control using the geometric constraints. The developed setup is shown in Fig. 4. A pair of Helmholtz coils and a pair of Maxwell coils are placed both along the x and y axes in order to control force working on the microrobot in two dimensions. A uniform magnetic field is generated by the Helmholtz coils, and a uniform magnetic field gradient is generated by the Maxwell coils. In the y axis, Maxwell coils are placed inside the Helmholtz coils. Designed parameters for the electromagnets are shown in Table I. The wire diameter is 0.2 mm, and the microrobot is composed of three $Nd_2Fe_{14}B$ magnets ($M=1.0\times10^6$ A/m, Grade N40, NeoMag Corp. , Japan). A high speed camera mounted with a microscopic lens (VW-6000, KEYENCE Corp. , Japan) is placed along the y axis to obtain the side view of the microrobot placed in a transparent tube of 8 mm in diameter as shown in Fig. 4.

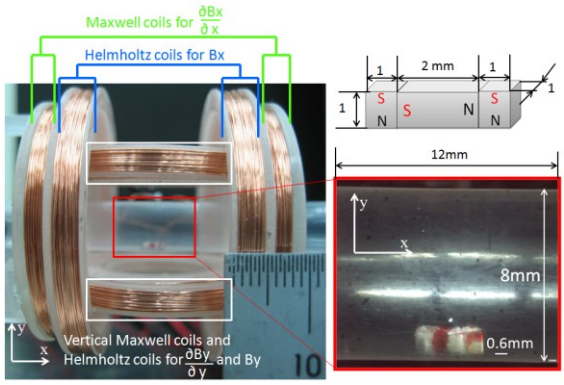

Fig. 4 Experimental setup for 2D magnetic driving of the microrobot using two-axis electromagnetic coils

TABLE I
PROFILES OF FOUR PAIRS OF COILS

Coils	Magnetic field at the center for a current of 1 [A]	Diameter [mm]	Coil Turns
X-axis Hz coils	6.5[mT]	40.4	145
X-axis Mx coils	440[mT/m]	34	186
Y-axis Hz coils	6.9[mT]	32	124
Y-axis Mx coils	1400[mT/m]	20	207

B. Experimental Result

Figure 5 shows the microrobot moving toward the upper surface of the internal wall of the tube. To lift the microrobot keeping its initial posture, a uniform gradient of the magnetic field in the y axis and a uniform magnetic field in the x axis were applied. When the microrobot reached the upper surface, the applied magnetic field was weakened.

Figure 6 shows the microrobot moving to the left and then the right in contact with the upper surface. When the microrobot reached the upper surface, a uniform gradient of the magnetic field in the x axis was applied to move the microrobot in a horizontal direction, while a uniform magnetic field in the y axis was applied for keeping the microrobot touched on the upper surface. The switching of motion from the left to the right was achieved by changing the direction of the magnetic field in the x axis. Although the posture of the microrobot became temporarily unstable when it reached the upper surface or the direction of motion was changed, the microrobot quickly recovered the posture and aligned itself along the tube.

From the experimental results, we confirmed the feasibility of the electromagnetic drive of the microrobot in 2D. Furthermore, the actuation of the microrobot was achieved by the simple control of switching the direction of the magnetic field.

IV. Model of Three-Dimensional Drive

A. 3D Geometric Constraint

The conditions where the microrobot moves in 3D along the vascular wall while keeping the contact need to be defined in the other two coordinate planes in addition to satisfying (1)-(4). In the 2D modeling and experiment, the microrobot was designed to be cuboid for easy prototyping; in 3D modeling, a column-shaped microrobot was used so that the rotation about the long axis is negligible in regards to the geometrical contact to the vascular wall. Fig. 7 depicts the 3D model of the microrobot placed on a vascular wall. The long direction of the microrobot coincides with the x axis, and the y axis passes through the contact point between the microrobot

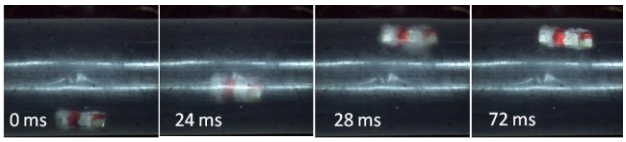

Fig. 5 The microrobot moving away from the lower surface and to the upper surface

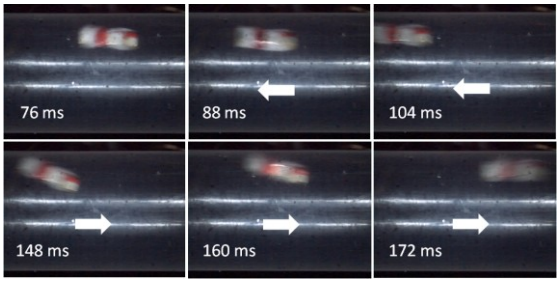

Fig. 6 The microrobot moving to the left and the right in contact with the upper surface

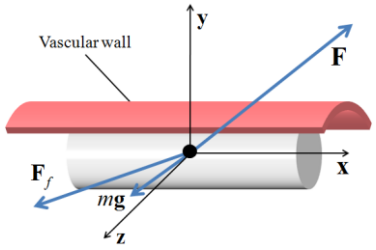

Fig. 7 3D model of microrobot placed on the wall with external magnetic force and fluid force applied

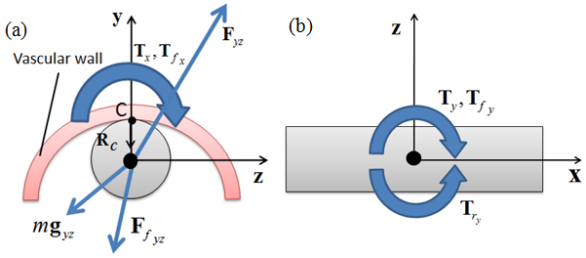

Fig. 8 (a)Cross-sectional model of the microrobot in the y-z plane. (b)Moments working on the microrobot in the z-x plane

and the vascular wall. Figure 8(a) shows the forces and the moments working on the microrobot in the y-z plane. $\mathbf{T}_i$ and $\mathbf{T}_{fi}$ denote the induced moments about the i axis by an external magnetic field and fluid force, respectively. The indexes of the force vectors indicate the projection to the planes. The conditions of the microrobot actuation in the y-z plane are described as:

$$\mu(\mathbf{F}+m\mathbf{g}+\mathbf{F}_f)\cdot\mathbf{e}_y-\left|(\mathbf{F}+m\mathbf{g}+\mathbf{F}_f)\cdot\mathbf{e}_z\right|>0 \quad (7)$$

$$\mathbf{T}_x+\mathbf{T}_{f_x}-(\mathbf{F}_{yz}+\mathbf{F}_{f_{yz}}+m\mathbf{g}_{yz})\times\mathbf{R}_c=\mathbf{0} \quad (8)$$

Equation (7) is the non-slip condition of the microrobot in the direction of the z axis. The force acting on the microrobot in the z axis needs to be smaller than the static friction to keep the contact position. Equation (8) is the non-rotation condition of the microrobot about the point C. This condition is expressed as an equality. Figure 9(b) shows the moments in the z-x plane. $\mathbf{T}_{ry}$ is the moment induced by the static friction about the y axis. The condition in the z-x plane is described as:

$$\left|\mathbf{T}_{r_y}\right|-\left|\mathbf{T}_y+\mathbf{T}_{f_y}\right|>0 \quad (9)$$

To prevent the rotation of the microrobot about the y axis, the total moment consisting of $\mathbf{T}_y$ and $\mathbf{T}_{fy}$ needs to be smaller than $\mathbf{T}_{ry}$.

B. 3D Magnetic Drive

The induced magnetic force and torque on the microrobot are explained in the following. Fig. 9 shows the columned-shaped design of the microrobot. The long direction of the microrobot coincides with the x axis, and the y axis passes through the contact point between the microrobot and the vascular wall. M is magnetization, and M_x and M_y are the components of magnetization in x-axis and y-axis, respectively. Figure 10(a) shows the magnetization of the microrobot when the microrobot is rotated about the x axis by

an angle of α. Induced magnetic force on the microrobot in the x-y-z coordinate system is described as:

$$\mathbf{F} = V \begin{bmatrix} M_x \\ M_y \cos\alpha \\ M_y \sin\alpha \end{bmatrix} \cdot (\nabla \mathbf{B}) \qquad (10)$$

Equation (10) indicates that there are three axial components of magnetization for α≠0. Thus, generating forces on the microrobot in the direction of each axis is theoretically possible.

Figure 10(b) shows the torque working on the microrobot. The x'-y'-z' coordinate system was obtained by a rotation of the x-y-z coordinate system about the x axis by an angle of α, followed by a rotation around the new z axis so that the new x' axis coincides with the magnetization of the microrobot. The torque in the x'-y'-z' coordinate system is expressed as:

$$\mathbf{T}' = V \begin{bmatrix} 0 \\ -\sqrt{M_x{}^2 + M_y{}^2}\, B_{z'} \\ \sqrt{M_x{}^2 + M_y{}^2}\, B_{y'} \end{bmatrix} \qquad (11)$$

In the x'-y'-z' coordinate system, the torque aligns the total magnetic moment with the induced magnetic field vector.

From above consideration, it is possible that three-axes magnetic forces and two-axis magnetic moments can be applied on the microrobot.

V. Discussion

The discussion in 2D suggests that the strict control of force and moment is not necessary for 2D actuation because the conditions are expressed as inequalities, allowing ranges of the input values. As long as the applied magnetic fields satisfy those inequalities, the desired motion of the microrobot can be achieved even if they are not precisely conrolled. In the case of axial magnetic propulsion of microrobot in a free 3D space, the locomotion condition is expressed as an inequality. The conditions to keep the position in the direction of the other two axes are expressed as equalities. The conditions preventing the rotation about in any axis are expressed as equalities. Thus, five out of the six conditions are expressed as equalities. On the other hand, in the proposed actuation utilizing geometric constraints as shown in Fig. 7, the three conditions of the microrobot about positioning are expressed as the inequalities (1), (2) and (7). The conditions for orientation are expressed as the equality (8) and the inequalities (3), (4) and (9). Five out of the six conditions are expressed as inequalities. Thus, easier control of the microrobot is possible compared with the free space control.

When the microrobot is controlled in the human body, tracking of the microrobot and the damage to the blood vessels by the microrobot should be considered. Target vessels and microrobot are in the order of a few millimeters. Thus, it can

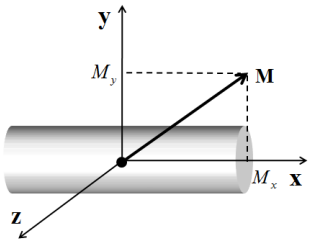

Fig. 9 Design of the simplified microrobot for moving along the blood vessel in 3D

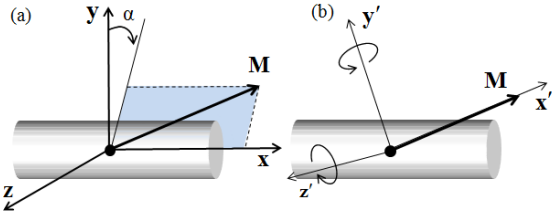

Fig. 10 (a) Magnetization of the micro robot on the coordinate system along the blood vessel wall.(b)Mechanism of torque acting on the micro robot on the coordinate system x' axis of which is coincident with the direction of the magnetization

be tracked by fluoroscopy. The order of the forces working on the microrobot is the same as that ofthe fluid force. Thus, the damage to the internal wall of the blood vessel is assumed to be sufficiently small.

VI. Conclusion

We proposed a concept of microrobotic actuation utilizing geometric constraints by the vascular wall. We modeled the force and torque working on the microrobot in 2D, and the 2D actuation of the microrobot placed in a tube was successfully demonstrated. We also expanded the model to 3D to clarify the conditions necessary for 3D actuation along the vascular path. Future work includes the development of the system capable of 3D actuation. Improved 3D control methods will be investigated, and the feasibility will be discussed considering the influence by the fluid force.

Acknowledgment

The authors thank Dr. A. Morita and Dr. M. Shojima for their advice, and Mr. S. Tottori for technical discussions.

References

[1] Michael P. Kummer, Jake J. Abbott, Bradley E. Kratochvil, Ruedi Borer, Ali SenguL, and Bradley J. Nelson, "OctoMag: AnElectromagnetic System for 5-DOF Wireless Micromanipulation," in *Proc. IEEE Int. Conf. Robotics and Automation*, 2010, pp. 1610-1615.

[2] S. Martel, J.-B. Mathieu, O. Felfoul, A. Chanu, E. Aboussouan, S. Tamaz, and P. Pouponneau, "Automatic navigation of an untethered device in the artery of a living animal using a conventional clinical magnetic resonance imaging system," *Applied Physics Lett*., vol. 90, no.11, pp. 114 105(1-3), 2007.

[3] Bradley J. Nelson, Ioannis K. Kaliakatsos and Jake J. Abbott, "Microrobots for Minimally Invasive Medicine," *Annu. Rev. Biomed. Eng.*, pp. 55-85, 2010. 12.

[4] Jongho Choi et. al., "Positioning of Microrobot in a Pulsating Flow using EMA System," in *Proc. 3rd IEEE RAS & EMBS Int. Conf. Biomedical Robotics and Biomechatronics*, 2010, pp. 588-593.